Inorganic Chemistry

Article

pubs.acs.org/IC

$Bi_2(IO_4)(IO_3)_3$: A New Potential Infrared Nonlinear Optical Material Containing $[IO_4]^{3-}$ Anion

Zhenbo Cao,[†,‡,§] Yinchao Yue,[†,‡] Jiyong Yao,[†,‡] Zheshuai Lin,[†,‡] Ran He,[†,‡,§] and Zhanggui Hu*[,†,‡]

[†]Key Laboratory of Functional Crystals and Laser Technology, Technical Institute of Physics and Chemistry, Chinese Academy of Sciences, Beijing 100190, P.R. China

[‡]Center for Crystal Research and Development, Technical Institute of Physics and Chemistry, Chinese Academy of Sciences, Beijing 100190, P.R. China

[§]Graduate University of the Chinese Academy of Sciences, Beijing 100049, P.R. China

Supporting Information

ABSTRACT: A new potential infrared (IR) nonlinear optical (NLO) material $Bi_2(IO_4)(IO_3)_3$ was synthesized by hydrothermal method. $Bi_2(IO_4)(IO_3)_3$ crystallizes in the chiral orthorhombic space group $P2_12_12_1$ (No. 19) with a = 5.6831(11) Å, b = 12.394(3) Å, and c = 16.849(3) Å. It exhibits a three-dimensional framework through a combination of the IO_3, IO_4, BiO_8, and BiO_9 polyhedra and is the first noncentrosymmetric (NCS) structure containing $[IO4]^{3-}$ anion. $Bi_2(IO_4)(IO_3)_3$ has an IR cutoff wavelength of 12.3 μm and belongs to the type 1 phase-matchable class with a moderately large SHG response of 5 × KDP, which is in good agreement with the theoretical calculations.

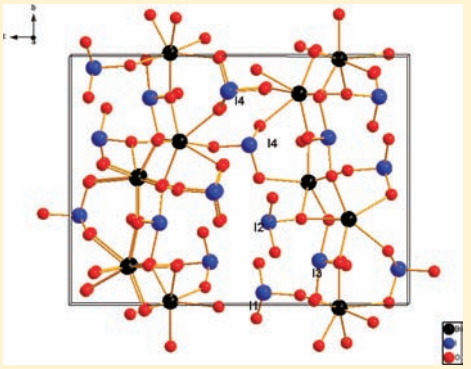

INTRODUCTION

Nonlinear optical (NLO) materials have important applications in laser frequency conversion, optical parameter oscillation (OPO), and signal communication.[1] According to their transparency ranges, NLO crystals can be divided into the ultraviolet (UV), visible, and infrared (IR) categories. Over the past few decades, several UV and visible NLO crystals, such as $KTiOPO_4$ (KTP),[2] $LiNbO_3$,[3] β-BaB_2O_4 (BBO),[4] and LiB_3O_5 (LBO),[5] have found practical applications. By contrast, IR NLO crystals, whether they are chalcopyrites represented by $AgGaX_2$ (X = S, Se) and $ZnGeP_2$ or halides like $CsGeBr_3$ and Tl_4HgI_6, have shortcomings of one kind or another that have seriously limited their applications.[6,7] Therefore, in the field of photoelectric functional materials chemistry, the search for new types of IR NLO crystals has attracted a great deal of research interest.[8−10]

We have been focused on metal iodates(V), a class of promising IR NLO materials. There are three iodate anions of pentavalent iodine: the widely studied $[IO_3]^-$ anion and recently studied $[IO_4]^{3-}$ and $[I_3O_8]^-$ anions.[11] Two inorganic compounds of $Ag_4(UO_2)_4(IO_3)_2(IO_4)_2O_2$ and $Ba[(MoO_2)_6(IO4)_2O_4]\cdot H_2O$ have been reported the observation of the $[IO_4]^{3-}$ anions,[12,13] but both of them crystallize in centrosymmetric (CS) structures with no second harmonic generation (SHG) response. $[I_3O_8]^-$ is a kind of polyiodate(V) formed from the condensation of three anions $[IO_3]^-$, containing both IO_3 and IO_4 polyhedra. Some anions of compounds, such as NaI_3O_8, α-$Cs_2(IO_3)(I_3O_8)$, β-$Cs_2(IO_3)(I_3O_8)$, and $Rb_2(IO_3)$-$(I_3O_8)(HIO_3)_2(H_2O)$, belong to the $[I_3O_8]^-$ ones.[11,14−16] Metal iodates(V) have been extensively studied in the 1970s by Bell Laboratories not only for their NLO properties, but also for their ferroelectric, piezoelectric, and pyroelectric properties.[17−23] More recently, a series of iodates with excellent SHG properties have been synthesized in succession, including $AMoO_3(IO_3)$ (A = Rb, Cs),[24] $A[(VO)_2(IO_3)_3O_2]$ (A = NH_4, Rb, Cs),[25] and $RE(MoO_2)(IO_3)_4(OH)$ [RE = Nd, Sm, Eu][26] by the Albrecht-Schmitt group; α-$Cs_2I_4O_{11}$,[15] $La(IO_3)_3$,[16] $NaYI_4O_{12}$,[16] and $A_2Ti(IO_3)_6$ (A = Li, Na)[27] by the Halasyamani group; $LiMoO_3(IO_3)$ by the Chen group;[28] and $BaNbO(IO_3)_5$,[29] $NaVO_2(IO_3)_2(H_2O)$[30] and $K(VO)_2O_2(IO_3)_3$[31] by the Mao group. These iodates show that the stereochemically active lone pair on the I(V) atom can be an asymmetric building unit producing a large SHG response. In addition, NaI_3O_8 and some heavy metal iodates, which are investigated by the Gautier-Luneau group, show a wide transparency range with IR cutoffs reaching 12 μm or longer wavelengths, thereby being a class of promising IR NLO material.[14,32,33]

Bismuth(III) is a heavy metal cation containing a lone electron pair like I(V), which in combination with the iodate anion can lead to both a large SHG response and a wide transparency range. However, two bismuth iodates, $Bi(IO_3)_3$

Received: September 10, 2011
Published: November 10, 2011

and $Bi(IO_3)_3{\cdot}2H_2O$, have been found to be CS with no SHG response.[34,35] Recently, we and Halasyamani's group have independently reported the same compound, namely, $BiO(IO_3)$,[36,37] which is synthesized by hydrothermal methods using excess HIO_3 and HNO_3 as the acid mineralizer, respectively. It displays a noncentrosymmetric (NCS) layered structure topology, containing layers of $(Bi_2O_2)^{2+}$ cations that are connected to $(IO_3)^-$ anions, and has a large SHG response.[36,37] In the present work, we report the synthesis, characterization, and electronic and NLO properties of a novel material in the Bi−I−O ternary system formulated as $Bi_2(IO_4)(IO_3)_3$ (**1**). Compound **1** has a three-dimensional (3D) framework, is the first NCS structure with $[IO_4]^{3-}$ anions, and produces a moderately strong SHG response of 5 × KH_2PO_4 (KDP) with an IR cutoff wavelength up to 12.3 μm.

EXPERIMENTAL SECTION

Materials and Methods. The chemicals used in this work were all AR grade and were purchased from commercial suppliers and used without further purification. Microprobe elemental analyses were performed on a Hitachi S-3500 SEM with an energy-dispersive X-ray spectroscope (EDS). Inductive-coupled plasma atomic emission spectrometry (ICP-AES) was performed on IRIS Intrepid II XSP (U.S. ThermoFisher) at 22 °C and a relative humidity of 18%. Powder X-ray diffraction patterns were recorded in the 2θ range of 5−70° with a scan step width of 0.02° using an automated Bruker D8 X-ray diffractometer equipped with a diffracted monochromator set for Cu K_α (λ = 1.5418 Å) radiation. Thermogravimetric analyses (TGA) and differential scanning calorimetric (DSC) analyses were performed under N_2 at a scan rate of 10 °C/min on a NETZSCH STA 449C analyzer. IR spectra were recorded on a Bruker Vertex 70 V spectrometer using the ATR technique with a ZnSe crystal in the range of 4500−600 cm^{-1} (2.2−16.7 μm). The UV−vis diffuse reflectance spectra were measured at room temperature with a Varian Cary 5000 UV−visible-NIR spectrophotometer in the range of 2500−250 nm (0.5−5 eV). The straightforward extrapolation method was used to deduce the band gap and absorption edge.[38] The SHG tests were carried out on the sieved powder samples by the Kurtz and Perry method[39] with a 1064 nm Q-switch Nd:YAG laser. The sample was ground and sieved into several distinct particle size ranges (0−50, 50−61, 61−90, 90−105, 105−125, 125−150, 150−200, and 200−300 μm). The KDP powders of similar particle size served as a reference to assume the effect. All of the samples were placed in separate tubes with two quartz glass sheets. No index-matching fluid was used in any of the experiments.

Synthesis of $Bi_2(IO_4)(IO_3)_3$. $Bi(NO_3)_3{\cdot}5H_2O$ (485.1 mg, 1 mmol), HIO_3 (527.7 mg, 3 mmol), HNO_3 (0.5 mL, ∼5 mmol), and 2.0 mL of deionized water were loaded into a 25 mL Teflon-lined autoclave and subsequently sealed. The autoclave was gradually heated to 215 °C in an oven, held for 5 d, and cooled slowly to room temperature at a rate of 10 °C/h. The final pH of the reaction system was about 0.5. Then the yellow mother liquor was decanted from the products, which were washed with 95% ethanol and deionized water and then air-dried. Colorless millimetric prismatic-like crystals (Figure S1 in the Supporting Information shows one of the crystals) were collected (425.0 mg, 75% yield based on Bi). The product purity was confirmed by powder X-ray diffraction analyses (see Figure S2 in the Supporting Information). EDS analyses of $Bi_2(IO_4)(IO_3)_3$ provided a Bi:I ratio of 1:1.99 (approximately equal to 2:4). ICP-AES elemental analyses showed a 36.67% content of Bi, which was in good agreement with 36.87% as determined by single crystal X-ray diffraction and EDS analyses.

Single Crystal Structure Determination. Single-crystal X-ray diffraction data were collected with the use of graphite-monochromatized Mo K_α (λ = 0.71073 Å) at 163 K on a Rigaku AFC10 diffractometer equipped with a Saturn CCD detector. Crystal decay was monitored by recollecting 50 initial frames at the end of data collection. The collection of the intensity data was carried out with the program Crystalclear.[40] Cell refinement and data reduction were carried out with the use of the program Crystalclear,[40] and face-indexed absorption corrections were performed numerically with the use of the program XPREP.[41] The structure was solved with the direct methods program SHELXS and refined with the least-squares program SHELXL of the SHELXTL.PC suite of programs. The final refinement included anisotropic displacement parameters for Bi and I atoms and a secondary extinction correction. The program STRUCTURE TIDY[42] was then employed to standardize the atomic coordinates. Additional experimental details are given in Table 1 and selected metrical data are given in Table 2. Further information may be found in Supporting Information.

Table 1. Crystal Data and Structure Refinements for $Bi_2(IO_4)(IO_3)_3$

formula	$Bi_2(IO_4)(IO_3)_3$
formula weight (g/mol)	1133.56
crystal system	orthorhombic
space group	$P2_12_12_1$ (19)
a (Å)	5.6831(11)
b (Å)	12.394(3)
c (Å)	16.849(3)
V (Å^3)	1186.8(4)
Z	4
T (K)	163(2)
Λ(Mo K_α) (Å)	0.71073
ρ_c (g/cm^3)	6.344
μ (mm^{-1})	40.089
crystal size (mm^3)	0.15 × 0.08 × 0.03
data/restraints/parameters	3775/0/107
Flack parameter	−0.012(4)
R1, wR2[a] [I > 2sigma(I)]	0.0258, 0.0529
R1, wR2 (all data)	0.0304, 0.0546

[a] $R1 = \sum||F_o| - |F_c||/\sum|F_o|$, $wR2 = \{\sum[w(F_o^2 - F_c^2)^2]/\sum w[(F_o)^2]^2\}^{1/2}$.

Table 2. Selected Bond Lengths (Å) of $Bi_2(IO_4)(IO_3)_3$[a]

$Bi_2(IO_4)(IO_3)_3$			
Bi(1)−O(3)#1	2.209(6)	I(1)−O(12)#6	1.794(6)
Bi(1)−O(11)#2	2.244(6)	I(1)−O(1)#6	1.807(6)
Bi(1)−O(7)#2	2.329(7)	I(1)−O(7)	1.836(7)
Bi(1)−O(10)#1	2.350(6)	I(2)−O(13)	1.803(6)
Bi(1)−O(6)#2	2.384(5)	I(2)−O(8)	1.819(6)
Bi(1)−O(8)#3	2.728(6)	I(2)−O(10)	1.830(6)
Bi(1)−O(2)#2	2.793(6)	I(3)−O(5)#7	1.807(6)
Bi(1)−O(5)#3	2.984(6)	I(3)−O(6)	1.884(6)
Bi(2)−O(3)	2.233(6)	I(3)−O(11)	1.983(6)
Bi(2)−O(9)#3	2.237(6)	I(3)−O(3)	2.102(6)
Bi(2)−O(6)	2.340(5)	I(4)−O(4)#5	1.801(6)
Bi(2)−O(11)#4	2.415(6)	I(4)−O(2)#5	1.811(6)
Bi(2)−O(4)	2.565(6)	I(4)−O(9)#5	1.883(6)
Bi(2)−O(8)	2.633(6)		
Bi(2)−O(12)	2.680(6)		
Bi(2)−O(7)#5	3.169(6)		
Bi(2)−O(5)#6	3.210(6)		

[a] Symmetry transformations used to generate equivalent atoms: #1 $x + 1/2, -y + 3/2, -z + 1$; #2 $-x + 3/2, -y + 2, z - 1/2$; #3 $x - 1/2, -y + 3/2, -z + 1$; #4 $-x + 1, y - 1/2, -z + 3/2$; #5 $-x + 2, y - 1/2, -z + 3/2$; #6 $-x + 2, y + 1/2, -z + 3/2$; #7 $-x + 1, y + 1/2, -z + 3/2$; #8 $-x + 3/2, -y + 1, z + 1/2$; #9 $-x + 3/2, -y + 2, z + 1/2$; #10 $x + 1, y, z$.

Theoretical Computations. The electronic properties are calculated by the plane-wave pseudopotential method[43] implemented

dx.doi.org/10.1021/ic201991m | Inorg. Chem. 2011, 50, 12818−12822

in the CASTEP package.[44] Ultrasoft pseudopotentials[45] are employed with the 6s and 6p electrons for bismuth and the 5s and 5p electrons for iodine. For oxygen, 1s electrons for oxygen are treated as the core electrons. The generalized gradient approximation (GGA) using the Perdew, Burke, and Ernzerhof (PBE) functional[46] are chosen for all the calculations. A kinetic energy cutoff of 500 eV and the Monkhorst-Pack *k*-point meshes[47] with a density of (4 × 2 × 1) in the Brillouin zone of the $Bi_2(IO_4)(IO_3)_3$ unit cell are used. Based on the electronic band structures, the refractive indices and SHG coefficients of the $Bi_2(IO_4)(IO_3)_3$ crystal are theoretically determined. The detailed calculation formulas are shown in ref 48.

RESULTS AND DISCUSSION

Synthesis. Repeated attempts have led us to find the optimum reaction conditions as indicated in Experimental Section. In addition, the replacements of HIO_3 with I_2O_5 or H_5IO_6 and of $Bi(NO_3)_3·5H_2O$ with Bi_2O_3 as starting materials also generated the target material. Some blue-black blocks of I_2(s) were observed as a byproduct, which was probably from the reduction of excess HIO_3 by water. Subsequently, the I_2 solids were removed by washing with ethanol.

Structure Description. $Bi_2(IO_4)(IO_3)_3$ crystallizes in a new structure (Figure 1) in noncentrosymmetric (NCS) space

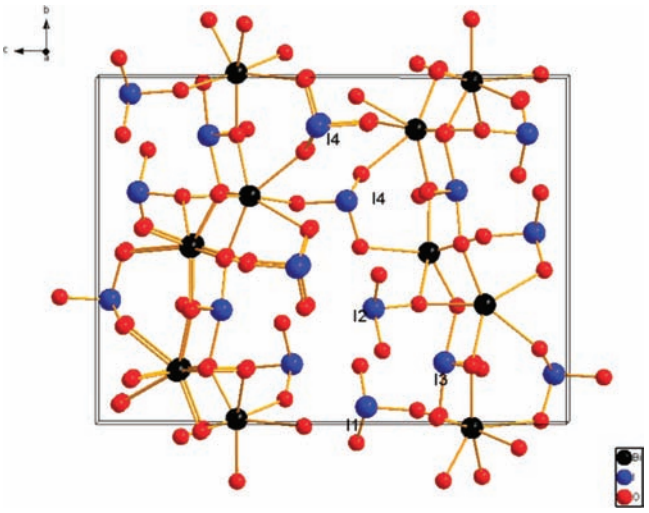

Figure 1. View of crystal structure of $Bi_2(IO_4)(IO_3)_3$ down the *a* direction.

group $P2_12_12_1$ (No. 19) of the orthorhombic system. The asymmetric unit contains two crystallographically independent Bi atoms, four independent I atoms, and thirteen independent O atoms. Figure 1 shows that I1, I2, and I4 are coordinated to a trigonal pyramid of three O atoms with the I−O distances ranging from 1.794(6) to 1.883(6) Å, which are comparable to those of $Bi(IO_3)_3$ (1.790(8)−1.828(8) Å)[34] and some other iodates containing IO_3 groups (1.777(6)−1.930(5) Å).[11] Furthermore, I3 is coordinated to four O atoms in a 'seesaw' environment with the I−O distances of 1.807(6)−2.102(6) Å, which are in agreement with those of 1.818(6)−2.054(6) Å in $Ag_4(UO_2)_4(IO_3)_2(IO_4)_2O_2$[12] and $Ba[(MoO_2)_6(IO4)_2O_4]·H_2O$. The coordination polyhedra of Bi1 and Bi2 cations are irregular with coordination numbers of 8 and 9 and Bi−O distances in the range of 2.209(6)−3.210(6) Å. These Bi−O distances are close to those of 2.387(7)−2.996(9) Å in $Bi(IO_3)_3$.[34] Selected bond distances are presented in Table 2, and the coordination environments of I1, I2, I3, and I4 are showed in Figure S3 in the Supporting Information. The bond valence sums (BVS) for the Bi1, Bi2, I1, I2, I3, and I4 atoms are 3.30, 3.04, 5.02, 4.95, 4.89, and 4.75, respectively.[49] It indicates that even if the Bi and I atoms are in different coordination environments, the oxidation states of +3 and +5 can be assigned to Bi and I atoms, respectively.

As shown in Figure 1, $Bi_2(IO_4)(IO_3)_3$ has a three-dimensional (3D) framework structure composed of the IO_3, IO_4, BiO_8, and BiO_9 polyhedra. The BiO_8 and BiO_9 polyhedra share corners and edges to form two-dimensional Bi−O layers parallel to the *ab* plane with the Bi1 and Bi2 atoms lying in chains along the *a* direction (Figure 2). I1, I2, and I3 atoms,

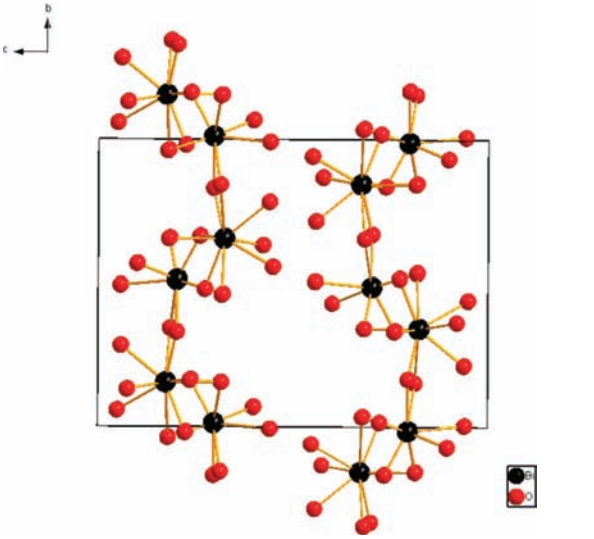

Figure 2. Layers composed by the BiO_8 and BiO_9 polyhedra parallel to the *ab* plane viewed down the *a*-axis.

which connect to the Bi atoms by bridging oxygen atoms, are attached to these layers, while I4 atoms further join these layers together by bridging oxygen atoms to form the 3D framework. As for the IO_3 and IO_4 groups themselves, they are all completely isolated from each other without any common O atoms. Two compounds of iodate $Ag_4(UO_2)_4(IO_3)_2(IO_4)_2O_2$ and $Ba[(MoO_2)_6(IO4)_2O_4]·H_2O$ contain isolated $[IO_4]^{3-}$ anions, but they both crystallize in centrosymmetric structures.[12,13] Other compounds containing both IO_3 and IO_4 polyhedra include NaI_3O_8, α-$Cs_2(IO_3)(I_3O_8)$, β-$Cs_2(IO_3)(I_3O_8)$ and $Rb_2(IO_3)(I_3O_8)(HIO_3)_2(H_2O)$. However, in all these compounds, the IO_3 and IO_4 groups are connected to form $[I_3O_8]^-$ anions.[11,14−16] $Bi_2(IO_4)(IO_3)_3$ is the first NCS structure that contains $[IO_3]^-$ and $[IO_4]^{3-}$ anions.

Thermal Studies. The TGA-DSC curves, as shown in Figure S4 in the Supporting Information, indicate that $Bi_2(IO_4)(IO_3)_3$ is thermally stable up to about 400 °C and displays three steps of weight loss, which are in agreement with the three endothermic peaks at 534, 570, and 845 °C, respectively. At 550 and 650 °C, the products of thermal decomposition should be $BiIO_4$[37] and α-Bi_5O_7I (JCPDS No. 01-071-3024), as confirmed by powder XRD studies (see Figures S5 and S6 in the Supporting Information). The experimental weight losses are in good agreement with calculated values (Supporting Information Figure S4). The residuals at 900 °C may be Bi_2O_3 by calculation, but collection

dx.doi.org/10.1021/ic201991m | *Inorg. Chem.* 2011, 50, 12818−12822

and analysis were difficult because they were in small amount and deposited on the walls of the Al_2O_3 crucible.

IR and UV−vis Diffuse Reflectance Spectra. IR spectra show five main peaks: 810 (ν_{I-O}, w), 748 (ν_{I-O}, s), 725 (ν_{I-O}, s), 692 (ν_{I-O}, s), 662 (ν_{I-O}, s) cm^{-1}, which are in good agreement with the I−O stretching vibrations in the regions of 600−840 cm^{-1}.[16,33] It indicates that $Bi_2(IO_4)(IO_3)_3$ is transparent in the range of 4500−813 cm^{-1} (2.2−12.3 μm) with IR cutoff wavelengths moving into the far-IR region (Figure S7 in the Supporting Information).

UV−vis Diffuse Reflectance Spectra shown in Figure 3 indicate that $Bi_2(IO_4)(IO_3)_3$ is a wide gap semiconductor with

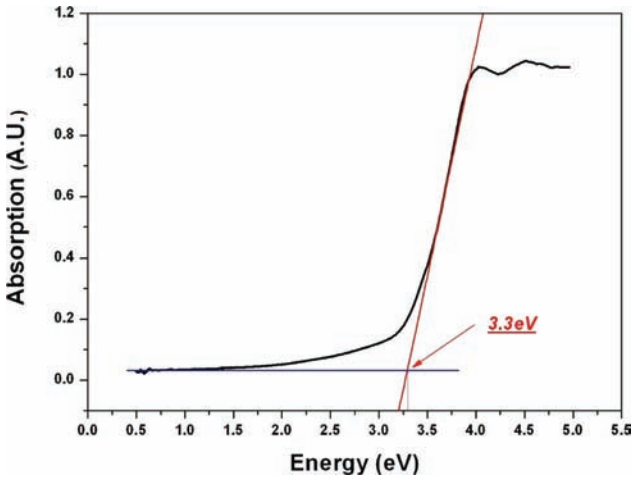

Figure 3. UV−vis diffuse reflectance spectra for $Bi_2(IO_4)(IO_3)_3$ with band gap of 3.3 eV.

an absorption edge of 376 nm and optical band gap of 3.3 eV. Band gaps have great influence on the laser damage threshold of IR NLO materials. With a large band gap, which is consistent with the crystal colorlessness, $Bi_2(IO_4)(IO_3)_3$ should have a high laser damage threshold.[10,50]

Second Harmonic Generation (SHG) Properties. Figure 4 shows the curves of the SHG signal intensity versus particle size

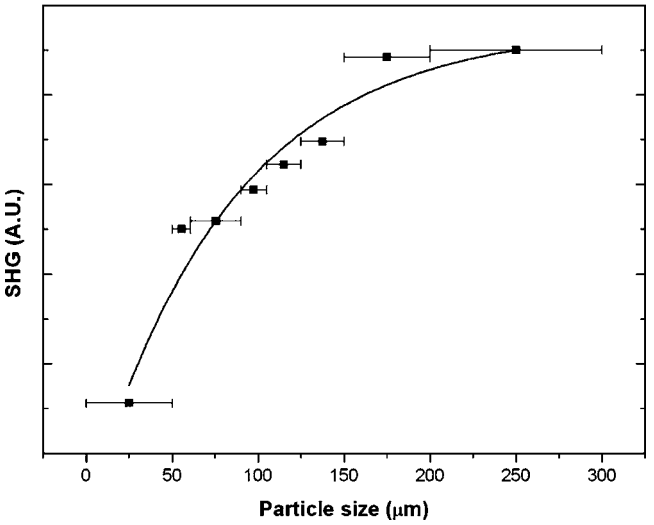

Figure 4. Phase-matching curve (Type 1) for $Bi_2(IO_4)(IO_3)_3$. The curve is to guide the eye and is not a fit to the data.

for ground $Bi_2(IO_4)(IO_3)_3$ crystals. For large particle sizes, the second harmonic intensity is independent of particle size. The tendency of the curve indicates that $Bi_2(IO_4)(IO_3)_3$ belongs to the type 1 phase-matching class according to the rules proposed by Kurtz and Perry.[39] Comparisons of the second harmonic signals produced by $Bi_2(IO_4)(IO_3)_3$ and KDP in the same particle range (150 to 200 μm) reveal that $Bi_2(IO_4)(IO_3)_3$ exhibits a moderately large SHG response of about 5 × KDP. The moderately large SHG efficiency is consistent with the electronic structure calculation.

Electronic Structure Calculation. The electronic band structures of $Bi_2(IO_4)(IO_3)_3$ are shown in Supporting Information Figure S8, along the lines of high symmetry points in the Brillouin zone. It is shown that $Bi_2(IO_4)(IO_3)_3$ is a direct gap crystal with the band gap of 3.17 eV, which is very close to the experimental value of 3.3 eV. The partial density of state (PDOS) projected on the constitutional atoms of the $Bi_2(IO_4)(IO_3)_3$ crystal is shown in Supporting Information Figure S9. Clearly, the valence band (VB) lower than −10 eV mainly consists of 2s orbitals for oxygen and 5s and 5p orbitals for iodine. The upper part of the VB from −10 to 0 eV is mainly composed of 2*p* orbitals of oxygen, 6s and 6p orbitals of bismuth and 5p orbitals of iodine, but the very top mostly consists of O 2p orbitals. There is significant hybridization between O 2p orbitals and I 5p orbitals, as well as Bi 6s and 6p orbitals. The bottom of the conduction band (CB) is composed of the orbitals of all atoms, and the p orbitals of I and Bi determine the CB minimum of $Bi_2(IO_4)(IO_3)_3$.

On the basis of the electronic band structure, the linear and nonlinear optical properties of $Bi_2(IO_4)(IO_3)_3$ have been calculated. It is shown that the linear refractive indices are n_x = 2.330, n_y = 2.526, and n_z = 2.414 at the radiation wavelength of 1064 nm. Clearly, the birefringence is quite large with Δn = 0.196, so this crystal is relatively easy to achieve the phase-matching conditions for the SHG light output. Meanwhile, the calculated SHG coefficient is d_{36} = −1.58 pm/V, which is very close to our experimental value of 5 times of KDP (d_{36} = 0.39 pm/V). Therefore, we conclude that $Bi_2(IO_4)(IO_3)_3$ is a promising NLO crystal, which can be applied in the IR region.

From the viewpoint of structural features, the strong anisotropic response (or birefringence) to the incident radiation is due to the large distortion of the BiO_8 and BiO_9 polyhedra and the presence of the lone-pair electrons on I atoms that occupy vertexes of the I−O triangular pyramids or quadrilateral pyramids. However, the spatial arrangement of those microscopic units is not regular, so the microscopic second-order susceptibilities of a group partly counteract those of another group, resulting in the decrease of the overall SHG effects. It is expected that if those active microscopic units could be aligned, the capability of this crystal to produce the larger nonlinear optical light output would be significantly improved. These structural understandings can give us some ideas to design NLO crystals with enhanced NLO effects.

CONCLUSION

In summary, a promising IR NLO material, $Bi_2(IO_4)(IO_3)_3$, has been prepared. It crystallizes in an acentric space group and displays a 3D framework composed of the IO_3, IO_4, BiO_8 and BiO_9 groups. Interestingly, it is the first time that the $[IO_4]^{3-}$ anion occurs in a noncentrosymmetric (NCS) compound of iodate. Moreover, the new compound is thermally stable, has a transparency range up to the beginning of the far-IR region, and displays intense SHG signals. On the basis of the SHG measurements on powders and theoretical calculations, $Bi_2(IO_4)(IO_3)_3$ readily

achieves the type 1 phase-matching conditions with a moderately large SHG response of approximately 5 × KDP. These findings have led us to conclude that this compound has potential applications as a quadratic NLO material. Further research on $Bi_2(IO_4)(IO_3)_3$ is in progress, which includes growing larger-size crystals and evaluating their optical properties such as refractive index, the Sellmeier equations, second-order NLO coefficients and the laser damage threshold.

■ ASSOCIATED CONTENT

Supporting Information

X-ray crystallographic file in CIF format, photograph of single crystal, simulated and experimental XRD patterns, picture of IO_3 and IO_4 polyhedra, TGA and DSC curves, XRD studies of the thermal decomposition for the compound, IR spectra, electronic band structure, and partial density of states of $Bi_2(IO_4)(IO_3)_3$ (PDF). This material is available free of charge via the Internet at http://pubs.acs.org.

■ AUTHOR INFORMATION

Corresponding Author

*E-mail: hu@mail.ipc.ac.cn.

■ ACKNOWLEDGMENTS

We thank Prof. Xiaotai Wang for helpful discussions.

■ REFERENCES

(1) Burland, D. M.; Miller, R. D.; Walsh, C. A. *Chem. Rev.* **1994**, *94*, 31−75.
(2) Driscoll, T. A.; Hoffman, H. J.; Stone, R. E.; Perkins, P. E. *J. Opt. Soc. Am. B: Opt. Phys.* **1986**, *3*, 683−686.
(3) Boyd, G. D.; Miller, R. C.; Nassau, K.; Bond, W. L.; Savage, A. *Appl. Phys. Lett.* **1964**, *5*, 234−236.
(4) Chen, C.; Wu, B.; Jiang, A.; You, G. *Sci. Sin. Ser. B* **1985**, *28*, 235−243.
(5) Chen, C.; Wu, Y.; Jiang, A.; Wu, B.; You, G.; Li, R.; Lin, S. *J. Opt. Soc. Am. B: Opt. Phys.* **1989**, *6*, 616−621.
(6) Schunemann, P. G. *AIP Conf. Proc.* **2007**, *916*, 541−559.
(7) Fernelius, N. C.; Hopkins, F. K.; Ohmer, M. C. *Proc. SPIE* **1999**, *3793*, 2−8.
(8) Kim, Y.; Seo, I.; Martin, S. W.; Baek, J.; Halasyamani, P. S.; Arumugam, N.; Steinfink, H. *Chem. Mater.* **2008**, *20*, 6048−6052.
(9) Zhang, G.; Qin, J. G.; Liu, T.; Li, Y. J.; Wu, Y. C.; Chen, C. T. *Appl. Phys. Lett.* **2009**, *95*, 261104−1−261104−3.
(10) Yao, J. Y.; Mei, D. J.; Bai, L.; Lin, Z. S.; Yin, W. L.; Fu, P. Z.; Wu, Y. C. *Inorg. Chem.* **2010**, *49*, 9212−9216.
(11) Gautier-Luneau, I.; Suffren, Y.; Jamet, H.; Pilmé, J. *Z. Anorg. Allg. Chem.* **2010**, *636*, 1368−1379.
(12) Bean, A. C.; Campana, C. F.; Kwon, O.; Albrecht-Schmitt, T. E. *J. Am. Chem. Soc.* **2001**, *123*, 8806−8810.
(13) Sykora, R. E.; Wells, D. M.; Albrecht-Schmitt, T. E. *Inorg. Chem.* **2002**, *41*, 2697−2703.
(14) Phanon, D.; Gautier-Luneau, I. *Angew. Chem., Int. Ed.* **2007**, *46*, 8488−8491.
(15) Ok, K. M.; Halasyamani, P. S. *Angew. Chem., Int. Ed.* **2004**, *116*, 5605−5607.
(16) Ok, K. M.; Halasyamani, P. S. *Inorg. Chem.* **2005**, *44*, 9353−9359.
(17) Nassau, K.; Shiever, J. W.; Prescott, B. E. *J. Solid State Chem.* **1973**, *7*, 186−204.
(18) Abrahams, S. C.; Sherwood, R. C.; Bernstein, J. L.; Nassau, K. *J. Solid State Chem.* **1973**, *7*, 205−212.
(19) Abrahams, S. C.; Sherwood, R. C.; Bernstein, J. L.; Nassau, K. *J. Solid State Chem.* **1973**, *8*, 274−279.
(20) Liminga, R.; Abrahams, S. C.; Bernstein, J. L. *J. Chem. Phys.* **1975**, *62*, 755−763.
(21) Abrahams, S. C.; Bernstein, J. L.; Nassau, K. *J. Solid State Chem.* **1976**, *16*, 173−184.
(22) Abrahams, S. C.; Bernstein, J. L. *Solid State Commun.* **1978**, *27*, 973−976.
(23) Svensson, C.; Abrahams, S. C.; Bernstein, J. L. *J. Solid State Chem.* **1981**, *36*, 195−204.
(24) Sykora, R. E.; Ok, K. M.; Halasyamani, P. S.; Albrecht-Schmitt, T. E. *J. Am. Chem. Soc.* **2002**, *124*, 1951−1957.
(25) Sykora, R. E.; Ok, K. M.; Halasyamani, P. S.; Wells, D. M.; Albrecht-Schmitt, T. E. *Chem. Mater.* **2002**, *14*, 2741−2749.
(26) Shehee, T. C.; Sykora, R. E.; Ok, K. M.; Halasyamani, P. S.; Albrecht-Schmitt, T. E. *Inorg. Chem.* **2003**, *42*, 457−462.
(27) Chang, H. Y.; Kim, S. H.; Ok, K. M.; Halasyamani, P. S. *J. Am. Chem. Soc.* **2009**, *131*, 6865−6873.
(28) Chen, X.; Zhang, L.; Chang, X.; Xue, H.; Zang, H.; Xiao, W.; Song, X.; Yan, H. *J. Alloys Compd.* **2007**, *428*, 54−58.
(29) Sun, C. F.; Hu, C. L.; Xu, X.; Ling, J. B.; Hu, T.; Kong, F.; Long, X. F.; Mao, J. G. *J. Am. Chem. Soc.* **2009**, *131*, 9486−9487.
(30) Yang, B. P.; Hu, C. L.; Xu, X.; Sun, C. F.; Zhang, J. H.; Mao, J. G. *Chem. Mater.* **2010**, *22*, 1545−1550.
(31) Sun, C. F.; Hu, C. L.; Xu, X.; Yang, B. P.; Mao, J. G. *J. Am. Chem. Soc.* **2011**, *133*, 5561−5572.
(32) Phanon, D.; Bentria, B.; Benbertal, D.; Mosset, A.; Gautier-Luneau, I. *Solid State Sci.* **2006**, *8*, 1466−1472.
(33) Phanon, D.; Mosset, A.; Gautier-Luneau, I. *Solid State Sci.* **2007**, *9*, 496−505.
(34) Bentria, B.; Benbertal, D.; Bagieu-Beucher, M.; Masse, R.; Mosset, A. *J. Chem. Crystallogr.* **2003**, *33*, 867−873.
(35) Phanon, D.; Gautier-Luneau, I. *Z. Kristallogr.: New Cryst. Struct.* **2006**, *221*, 243−244.
(36) Nguyen, S. D.; Yeon, J.; Kim, S. H.; Halasyamani, P. S. *J. Am. Chem. Soc.* **2011**, *133*, 12422−12425.
(37) Cao, Z. B.; Yue, Y. C.; Hu, Z. G. *J. Synth. Cryst* **2011**, *40*, 858−861.
(38) Schevciw, O.; White, W. B. *Mater. Res. Bull.* **1983**, *18*, 1059−1068.
(39) Kurtz, S. K.; Perry, T. T. *J. Appl. Phys.* **1968**, *39*, 3798−3813.
(40) Rigaku. *CrystalClear*; Rigaku Corporation, Tokyo, Japan, 2008.
(41) Sheldrick, G. M. *Acta Crystallogr., Sect. A: Found. Crystallogr.* **2008**, *64*, 112−122.
(42) Gelato, L. M.; Parthe, E. *J. Appl. Crystallogr.* **1987**, *20*, 139−143.
(43) Payne, M. C.; Teter, M. P.; Allan, D. C.; Arias, T. A.; Joannopoulos, J. D. *Rev. Mod. Phys.* **1992**, *64*, 1045−1097.
(44) Clark, S. J.; Segall, M. D.; Pickard, C. J.; Hasnip, P. J.; Probert, M. I. J.; Refson, K.; Payne, M. C. *Z. Kristallogr.* **2005**, *220*, 567−570.
(45) Vanderbilt, D. *Phys. Rev. B: Condens. Matter* **1990**, *41*, 7892−7895.
(46) Perdew, J. P.; Burke, K.; Ernzerhof, M. *Phys. Rev. Lett.* **1996**, *77*, 3865−3868.
(47) Monkhorst, H. J.; Pack, J. D. *Phys. Rev. B: Condens. Matter* **1976**, *13*, 5188−5192.
(48) Chen, C. T.; Lin, Z. S.; Wang, Z. Z. *Appl. Phys. B: Lasers Opt.* **2005**, *80*, 1−25.
(49) Brown, I. D.; Altermatt, D. *Acta Crystallogr. Sect. B: Struct. Sci.* **1985**, *41*, 244−247.
(50) Lin, X.; Zhang, G.; Ye, N. *Cryst. Growth Des.* **2008**, *9*, 1186−1189.